

Effect of Sn Addition to Pt/CeO₂-Al₂O₃ and Pt/Al₂O₃ Catalysts: An XPS, ¹¹⁹Sn Mössbauer and Microcalorimetry Study

J. C. Serrano-Ruiz¹, G.W. Huber², M.A. Sánchez-Castillo², J.A. Dumesic², F. Rodríguez-Reinoso¹ and A. Sepúlveda-Escribano^{1,*}

¹*Departamento de Química Inorgánica. Universidad de Alicante, Apartado 99, E-03080 Alicante, Spain.*

²*Department of Chemical Engineering. University of Wisconsin-Madison, Madison, WI 53706 USA*

*Corresponding author

E-mail address: asepul@ua.es (A. Sepúlveda-Escribano)

Fax: +34 965 90 34 54;

Tel: +34 965 90 39 74

Abstract

The effect of Sn addition to Pt/CeO₂-Al₂O₃ and Pt/Al₂O₃ catalysts was studied with X-ray photoelectron spectroscopy (XPS), ¹¹⁹Sn Mössbauer spectroscopy and adsorption microcalorimetry of CO at room temperature. Catalysts were reduced *in situ* at 473 (“non-SMSI state”) and 773 K (“SMSI state”). ¹¹⁹Sn Mössbauer and XPS results indicated that the presence of cerium in bimetallic catalysts inhibited reduction of tin. Furthermore, it was found that tin facilitated reduction of cerium (IV) to cerium (III). Microcalorimetric analysis indicated that cerium addition caused the appearance of a more heterogeneous distribution of active sites, whereas tin addition led to a higher homogeneity of these sites. Reduction at 773 K decreased the Pt surface area as measured by CO chemisorption for all catalysts used in this study. Tin addition to Pt/Al₂O₃ and Pt/CeO₂-Al₂O₃ also decreased the Pt surface area due to formation of PtSn and possibly Pt-SnO_x species. Cerium addition to Pt/Al₂O₃ caused a loss of Pt surface area only when the catalyst was reduced at 773 K, presumably due to migration of the reduced cerium onto Pt particles. Cerium addition to Pt/Al₂O₃ caused an increase in the catalytic activity for crotonaldehyde hydrogenation, whereas Sn addition to Pt/Al₂O₃ decreased the activity of Pt/Al₂O₃ catalysts. Higher reduction temperature caused an increase in the initial catalytic activity for crotonaldehyde hydrogenation for all the catalysts studied. Selectivity enhancements for crotyl alcohol formation in

crotonaldehyde hydrogenation were observed for the Ce and Sn promoted catalysts after a reduction at 773 K.

Keywords: Pt-Sn catalysts, CeO₂, crotonaldehyde hydrogenation, adsorption calorimetry, Mössbauer, XPS.

1. INTRODUCTION

The effects of so-called strong metal-support interactions (SMSI) have received considerable attention ever since the original discovery by Tauster, et al. [1], and these effects induced by high temperature reduction treatments (typically $T_{\text{redn}} \geq 723$ K) are generally considered to be associated with reducible supports such as TiO_2 [2], NbO_5 [3] and, especially CeO_2 [4,5]. Catalysts supported on reducible oxides have shown interesting catalytic and chemisorption properties, such as a decrease in H_2 chemisorption ability [6], suppression of alkane hydrolysis activity, increase in CO hydrogenation activity [7], and improvement in selectivity of crotyl alcohol for crotonaldehyde hydrogenation [8-10] when catalysts are subjected to high temperature reduction (> 773 K). Electron microscopy studies have shown that after high temperature reduction, partially reduced oxide species migrate, and decorate the metal surface [4-6,11,12]. Bernal, et al. have shown that in the case of a Pt/ CeO_2 catalyst this decoration occurs at a reduction temperature of 973 K and CePt_5 particles are formed at temperatures of 1173 K [13]. This decoration effect occurs at lower temperatures for Metal/ TiO_2 systems, and Datye, et al. have postulated that the SMSI effect is different for Metal/ TiO_2 and Metal/ CeO_2 systems [7]. Using HRTEM they observed that Pt clusters grew in an epitaxial relation on CeO_2 , whereas reduced TiO_2 particles migrated onto Pt clusters when catalysts were reduced at 773 K. This result has been confirmed by Abid, et al. who also observed that Pt particles 3-4 nm in size grew in an epitaxial pattern on ceria after reduction at 773 K [14]. Thus, it is possible that CeO_x is able to modify the geometric properties of Pt [14].

The existence of metal-support interactions can be assessed with the help of probe reactions such as hydrogenation reactions, for which both the activity and the selectivity are generally dependent on the catalyst reduction. One of the most interesting reactions is the hydrogenation of α,β unsaturated aldehydes [8,9]. This reaction can produce the saturated aldehyde (through the hydrogenation of the C=C bond) or the unsaturated alcohol (through the hydrogenation of the carbonyl C=O bond). The former reaction is favored on unpromoted platinum catalysts from both thermodynamic and kinetic points of view. However, the use of reducible supports such as CeO_2 produces an important enhancement in the selectivity toward the unsaturated alcohols [10,14]. For example, Englisch, et al. [41] observed that TiO_x species migrated onto Pt particles after high temperature reduction (773 K), leading to an improvement in catalyst activity

and selectivity towards crotyl alcohol in crotonaldehyde hydrogenation. They concluded that this increase in activity was probably due to crotonaldehyde adsorption at interfacial Pt-TiO_x sites.

The hydrogenation of crotonaldehyde on Pt has been shown to be structure sensitive, where the selectivity and activity is a function of Pt metal particle size [41]. Theoretical [42] and single crystal studies [47] indicate that the adsorption structures of α,β -unsaturated aldehydes depend on the metal surface planes. Beccat, et al. have shown that Pt(111) exhibits some selectivity to crotyl alcohol, while the other low-index Pt surface did not make any crotyl alcohol [47]. Englisch, et al. concluded that increasing the abundance of Pt(111) surfaces in a catalyst can increase the selectivity to crotyl alcohol [41].

The addition of a second metal to noble metal catalysts can modify catalytic behavior, such as in the case of bimetallic Pt-Sn catalysts used for dehydrogenation processes [15,16] or for hydrogenation of α,β unsaturated aldehydes [17]. Tin addition to Pt catalysts has been shown to improve the selectivity of crotyl alcohol for crotonaldehyde hydrogenation [18,19].

In spite of the great amount of research devoted to the SMSI effect, a very low number of studies have reported the effect of adding a second non active metal to catalysts supported on reducible oxides. In these complex systems, the role of the reducible oxide in determining the chemical nature of the second metal species is especially important, as it determines the degree and kind of the interactions that can take place with the noble metal, this conditioning its catalytic properties in a great number of interesting reactions (selective hydrogenations, alkane dehydrogenation, etc.).

In this paper we report a pioneer study on the presence of two promoters, tin and ceria, in a Pt based catalysts, and the effect of reciprocal interactions between these species have been followed by a great number of characterization techniques. The main objective was to analyze the effect of reduction temperature on Pt/CeO₂-Al₂O₃ catalysts and to analyze how catalytic properties change by the presence of a second non active metal such as Sn, in a given Pt/Sn atomic ratio. Various techniques (XPS, adsorption microcalorimetry and Mössbauer spectroscopy) were used to characterize catalysts reduced at 473 K (non-SMSI state) and 773 K (SMSI state) to study this effect. In addition, hydrogenation of crotonaldehyde was used as a probe reaction to complete the

results obtained in the characterization section. To our knowledge, this is the first time that a so comprehensive study on this kind of systems has been reported.

2. EXPERIMENTAL

Catalysts preparation

The starting support was a commercial γ -Al₂O₃ (Puralox SCCa 150/200, from SASOL), with a BET surface area of 228 m² g⁻¹ (N₂, 77K). The CeO₂-Al₂O₃ support was prepared by impregnation of the γ -Al₂O₃ with an aqueous solution of Ce(NO₃)₃·6H₂O (from Aldrich, 99%) of the appropriate concentration to load 25 wt % CeO₂ (5 ml. of solution per gram of γ -Al₂O₃). The slurry formed was stirred at room temperature for 24 h, and the excess solvent was removed by heating at 353 K for 2 h. The solid obtained was dried overnight at 383 K followed by calcination at 673 K for 6 h, with a heating rate of 2 K min⁻¹. The CeO₂-Al₂O₃ support had a BET surface area of 153 m² g⁻¹ (N₂, 77 K).

The monometallic catalysts, Pt/Al₂O₃ and Pt/CeO₂-Al₂O₃, were prepared by impregnation of the supports with aqueous solutions of [Pt(NH₃)₄](NO₃)₂ (from Aldrich, 99%). The solids were dried overnight at 383 K and then calcined in air at 673 K for 6 h. The bimetallic catalysts, Pt-Sn/Al₂O₃ and Pt-Sn/CeO₂-Al₂O₃, were prepared by successive impregnation. The supports were first impregnated with aqueous nitric acid solutions of Sn(C₂O₄) (from Aldrich, 98%), and the samples were then dried at 383 K and calcined at 673 K for 6 h. The Pt and Ce were subsequently added to the SnO_x/Al₂O₃ using the same preparation route as mentioned above. The amount of tin loaded corresponded to an atomic Pt/Sn ratio of 1:1. The actual metal content of the catalysts was determined by ICP measurements as reported in Table 1.

Catalysts Characterization

X-ray photoelectron spectra (XPS) were acquired with a VG-Microtech Multilab 3000 spectrometer equipped with a hemispherical electron analyzer and a Mg K α (h=1253.65 eV, 1eV=1.6302 x 10⁻¹⁹ J) 300-W X-ray source. The powder samples were pressed into small Inox cylinders and then mounted on a sample rod placed in a pre-treatment chamber and reduced in flowing H₂ for 1h at 473 and 773 K before being transferred to the analysis chamber. Before recording the spectra, the sample was

maintained in the analysis chamber until a residual pressure of ca. 5×10^{-7} N·m² was reached. The spectra were collected at a pass energy of 50 eV. The intensities were estimated by calculating the integral of each peak, after subtraction of the S-shaped background, and by fitting the experimental curve to a combination of Lorentzian (30%) and Gaussian (70%) lines. All binding energies were referenced to the C 1s line at 284.6 eV, which provided binding energy values with an accuracy of ± 0.2 eV.

Room temperature Mössbauer spectra of ¹¹⁹Sn were collected using an Austin Science Associates Model S-600 Mössbauer spectrometer connected to a microcomputer with a PCAII data collection board. The spectrometer was operated in the constant-acceleration mode, with a 10-mCi single-line γ -ray source of Ca^{119m}SnO₃ (Amarsham). Detection of the 23.88 KeV γ rays was achieved with a Xe-CO₂ proportional counter. A 0.05-mm-thick Pd foil was placed between the source and detector to filter 25.04 and 25.27-KeV X rays from the source. A 50/50 mixture of BaSnO₃ and β -Sn powder was used to calibrate the magnitude and linearity of the Doppler velocity for our system. Chemical shifts are reported relative to BaSnO₃ at room temperature. The catalysts were reduced at 473 K and 773 K before collecting the spectra using hydrogen (Liquid Carbonic) purified by passing through a bed of molecular sieves (13X) at 77K during 5 hours.

Differential heats of CO adsorption were measured at 300 K in a Setaram BT2.15D heat-flux calorimeter using the method described in detail elsewhere [12]. This calorimeter was connected to a high vacuum (base pressure $<10^{-6}$ Torr) volumetric system employing Baratron capacitance manometers for precision pressure measurement ($\pm 0.5 \times 10^{-4}$ Torr). The maximum apparent leak rate of the volumetric system (including the calorimetric cells) was 10^{-6} Torr·min⁻¹ in a system volume of approximately 70 cm³ (i.e. 10^{-6} μ mol·min⁻¹). The procedure for microcalorimetric measurements used in this study is described below: each sample (about 0.25 g.) was treated ex situ in ultrapure hydrogen (99.999% with further purification, AGA) for 5 hours (2 K·min⁻¹ ramp, 100 ml·min⁻¹) at the desired temperature (473 or 773 K) and then the sample was purged for 1h at the same temperature in ultrahigh purity helium (99.999% with further purification, AGA) in order to remove adsorbed hydrogen. Then it was sealed in a Pyrex NMR tube capsule and broken in a special calorimetric cell [20] after the sample had attained thermal equilibrium with the calorimeter. After the capsule was broken, the microcalorimetric data were collected by sequentially introducing small

doses (1-10 μmol) of CO (99.5% with further purification, AGA) onto the sample until it became saturated. The resulting heat response for each dose was recorded as a function of time and integrated to determine the energy released (mJ). The amount of gas adsorbed (μmol) was determined volumetrically from the dose, equilibrium pressures, and the system volumes and temperatures. The time required for the pressure to equilibrate in the calorimeter after each dose was approximately 1-15 min., and the heat response was monitored for 20-30 min after each dose to ensure that all heat was detected and to allow the heat response to return to the baseline value. The differential heat ($\text{kJ}\cdot\text{mol}^{-1}$), defined as the negative of the enthalpy change of adsorption per mole of gas adsorbed, was then calculated for each dose by dividing the heat released by the amount adsorbed.

The catalytic behavior of the samples in the vapor-phase hydrogenation of crotonaldehyde (2-butenal) was tested in a U-shaped quartz microflow reactor at atmospheric pressure under differential conditions. Before each reaction run, the catalyst (around 0.15 g) was reduced *in situ* at 473 and 773 K under flowing hydrogen ($50\text{ cm}^3\cdot\text{min}^{-1}$) for 5 h and then cooled under hydrogen to the reaction temperature, 353 K. Then, it was contacted with a reaction mixture (total flow: $50\text{ cm}^3/\text{min}$, H_2/CROALD ratio of 26) containing purified hydrogen and crotonaldehyde (Fluka, 99.5 %) which was prepared by passing a hydrogen flow through a thermostabilized saturator (293 K) containing the unsaturated aldehyde. The concentration of the reactants and the products at the outlet of the reactor was determined by online gas chromatography with a Carbowax 20 M 58/90 semicapillary column.

3. RESULTS AND DISCUSSION

X-ray photoelectronic spectroscopy

The chemical species present on the catalysts surfaces and their proportions were evaluated by XPS. The energy regions of Ce 3d, Sn $3d_{5/2}$ and Pt $4d_{5/2}$ core levels in calcined and reduced (at 473 and 773 K) samples were recorded. Although the most intense photoemission lines of platinum were those arising from the Pt 4f levels, this energy region became overshadowed by the presence of a very strong Al 2p peak, and the Pt 4d lines were thus analyzed instead [21,22]. The fresh calcined samples showed an asymmetric broad Pt $4d_{5/2}$ peak (Figure 1). It could be resolved, after curve fitting

procedures, into three components with binding energies of 317.9-318.7, 316.1-316.8 and 314.3-314.8 eV. The two components at higher binding energies can be ascribed to PtO₂ species [23,24] created after the calcination process, while the third band at lower binding energies can be assigned to the presence of Pt(II) species. This assignment of the Pt oxidation state is difficult, and data in the literature are contradictory. Furthermore, the low levels of Pt present in the samples, and the broad nature of the Pt 4d features, introduced considerable uncertainty into the determination of binding energies. It is interesting to observe that the Pt 4d_{5/2} BE values of the samples containing ceria are shifted to higher values (Figure 1). The observed shift in binding energies may be the consequence of interaction with the cerium phase, leading to an electronic polarization of the platinum precursor clusters. This result is not in agreement with the work reported by Navarro et al. [22] where a shift to lower binding energies was found in cerium-containing platinum catalysts. However, it has been found that this shift in BE created by the interaction of platinum particles with ceria is strongly dependent of the cerium content of the catalysts [25]. Thus, catalysts with high cerium content (as those of the present study) showed higher Pt 4d_{5/2} BE, while platinum particles in catalysts with low cerium content seemed to be slightly more reduced than in the corresponding cerium-free counterpart [25].

The chemical changes in the platinum particles after reduction in H₂ at 473 and 773 K were also investigated by XPS. The Pt 4d_{5/2} spectra for the calcined and the reduced samples are shown, as a representative sample in Figure 2, for the Pt/CeO₂-Al₂O₃ catalyst. The Pt 4d_{5/2} binding energies for all the catalysts under study, with the corresponding contribution to the overall signal in brackets, are included in Table 2. The XPS spectra indicate a shift of the Pt 4d_{5/2} binding energies toward lower values as the reduction temperature is increased. It is interesting to observe the appearance of a band centered around 313.0 eV in reduced samples, which is indicative of the presence of Pt⁰ species in agreement with results reported by Shyu, et al. [23]. It should be noted that in all catalysts studied, even after reduction at 773 K, platinum seems to maintain some δ⁺ character (or even stay as oxidized Pt(II) species) indicating a strong platinum-support interaction.

The Sn 3d_{5/2} spectra for the fresh and reduced in situ catalysts are compared in Figure 3. XPS spectra indicate a shift of the Sn 3d_{5/2} binding energy toward lower values as the reduction temperature increases in both cases, which is indicative of tin reduction. The results for the cerium-free Pt-Sn/Al₂O₃ catalyst (Figure 3a) showed one

asymmetric spectrum, which is probably due to the sum of two different contributions (Sn^{ox} (II and IV) and $\text{Sn}(0)$) to the overall signal. In the case of the unreduced catalyst, one small band appeared at 485.2 eV which may be ascribed to Sn(II) species, although most of the tin contribution was due to one band centered at 486.8 eV, characteristic of Sn(IV). The weight of this band at high B.E. in the overall signal decreased with reduction temperature and one peak appeared centered at 484.7 eV. This contribution has been ascribed in the literature to reduced Sn^0 [17,26]. The intensity of this peak increased with reduction temperature (from 8 to 18 % of the overall signal) indicating a higher amount of metallic tin after reduction at high temperature. However, reduction of tin was not complete and oxidized tin species were detected even after reduction at 773 K, in agreement with previous results on alumina-supported catalysts [27-29]. It is difficult to discriminate between Sn(II) and Sn(IV) with XPS. The objective of the deconvolution was mainly to separate the contribution of oxidized tin species (both Sn(II) and Sn(IV)) from the contribution of metallic tin. It has been found that the $\text{Sn}^{\text{ox}}/\text{Sn}_{\text{total}}$ ratio depends, among others factors, on the type of support [27]. When silica or carbon are used as catalyst support their inertness favors the interaction between platinum and tin making it possible to achieve reduction of Sn particles at moderate temperatures [16,19,30,31]. When alumina is used as a support, it interacts strongly with the Sn and hinders the reduction of SnO. [32-34].

The spectra obtained with the cerium-containing bimetallic catalyst Pt-Sn/CeO₂-Al₂O₃ (Figure 3b) had a Gaussian shape. After calcination and reduction at 473 K, no reduced tin species were detected (Figure 3b). In contrast, the cerium-free catalysts contained a small amount of reduced Sn (8 %) after reduction at 473 K. Only after reduction at high temperature (773 K) did Sn^0 (centered at 484.4 eV) appear for the Pt-Sn/CeO₂-Al₂O₃ catalyst. The reduced Sn species had a weight contribution of 16 % of the Sn species, which is slightly lower than in the cerium-free catalyst (18 %). As it has been noted above, the extent of reduction of tin strongly depends on support. It seems that the presence of cerium modified the Sn-alumina interaction, stabilizing the oxidized tin species. In this way, Del Angel, et al. [35], modified Pt-Sn/Al₂O₃ catalysts with the reducible oxide La₂O₃ and observed a decrease in the metallic tin amount with increasing La content for catalysts reduced at 573 K.

Cerium 3d XPS spectra have been analyzed for Pt/CeO₂-Al₂O₃ and Pt-Sn/CeO₂-Al₂O₃ catalysts both after calcination and after *in situ* reduction at 473 and 773 K. This complex spectrum (not shown) was analyzed by fitting two sets of spin multiplets,

corresponding to the $3d_{3/2}$ y $3d_{5/2}$ contributions, labeled as u and v , respectively, and using up to four peaks from each contribution [36]. The percentages of CeO_2 reduction after the different treatments have been determined taking into consideration the relative intensity of the peaks which are representative of Ce (III) in the total Ce 3d region [9]. The values obtained have been plotted in Figure 4 and are reported in Table 2. It can be seen that the extent of Ce (IV) reduction increases with reduction temperature. There is a certain amount of Ce (III) even in the fresh (calcined) catalysts, which is probably due to photoreduction of Ce (IV) ions during XPS experiments also reported by Mastelaro, et al [37]. The extent of Ce (IV) reduction is higher in the case of the bimetallic catalyst for the two reduction temperatures used in this work. This result indicates that, as seen in the Sn XPS spectra, the Sn and Ce are interacting. After reduction at 473 K both catalysts showed similar levels of cerium reduction (around 38%); however, when catalysts were reduced at 773 K, the bimetallic catalyst showed a higher amount of reduced cerium (46%) than its monometallic counterpart (39%). This effect of second metal in cerium reducibility has been observed before for Pt-Zn/ CeO_2 - SiO_2 catalysts [9]. It seems that the presence of tin facilitates H_2 transport from the platinum surface to the ceria support.

It can be seen in Table 2 that the Pt/Al XPS atomic ratio, which can be considered a measure of the platinum dispersion on the support, decreased with reduction temperature for all catalysts prepared except for Pt/ Al_2O_3 . Thus, platinum does not appreciably sinter after reduction treatment. In the case of Pt-Sn/ Al_2O_3 , the observed decrease in Pt/Al atomic ratio is accompanied by a decrease in Pt/Sn values. As the reduction temperature is increased, the tin decreases the platinum surface area by forming an alloy or by covering with oxidized tin species for the Pt-Sn/ Al_2O_3 catalyst. Increasing the reduction temperature decreased the Pt/Ce atomic ratio and increased the Ce/Al for the Pt/ CeO_2 - Al_2O_3 catalyst. This result suggests that during reduction the cerium ions can migrate onto platinum particles, which could account for the decrease in Pt/Al atomic ratio in monometallic Pt/ CeO_2 - Al_2O_3 catalyst. Pt-Sn/ CeO_2 - Al_2O_3 showed lower Ce/Al atomic ratios than the monometallic counterpart. This behavior again can be attributed to the coverage of ceria (or partially reduced ceria) particles by oxidized tin species with a strong interaction with the support.

Tin Mössbauer Spectroscopy

The oxidation state of Sn as a function of reduction temperature was studied in more detail by ^{119}Sn Mössbauer spectroscopy. Figure 5 shows the room temperature spectra for bimetallic catalysts after reduction at 473 and 773 K. The fitting parameters of these spectra are shown in Table 3. The Pt-Sn/ Al_2O_3 (Figure 5a) spectrum after reduction at 473 K showed one small doublet characteristic of Sn^{2+} (20% area) and one large band (80 % area) at an isomer shift of 0 mm/s typical of Sn^{4+} species. After reduction at 773 K the Sn^{4+} species decreased (7 % area) while the relative area due to Sn^{2+} increased from 20 to 62 %. It should be noted that the chemical composition of the Sn species is not strictly proportional to the relative area in the Mössbauer spectra because of differences in the recoil-free fractions. The high temperature reduction treatment also resulted in the appearance of a singlet peak (31 % area) at an isomer shift of 2.33 mm/s, which can be assigned to metallic tin alloyed with platinum [16]. These results are consistent with the XPS results, indicating that a high-temperature reduction is required to reduce the Sn species. The Sn^{2+} species could be Sn species that is interacting with alumina.

The spectrum for Pt-Sn/ CeO_2 - Al_2O_3 (Figure 5b) reduced at 473 K is similar to that of the cerium-free catalyst although, in this case, more Sn^{4+} is detected (93%). After the treatment at high temperature (773 K) the spectrum consisted principally of Sn^{2+} (69 %) and a lower amount of metallic tin (21 %). The average oxidation state of tin was higher than in the cerium-free catalyst (1.7 vs 1.5). In this case the Sn^{2+} species could be interacting with both alumina and ceria. These results are consistent with XPS measurements which show that oxidized tin species are more difficult to reduce when cerium is present on the alumina support. The XPS and Mössbauer data indicate that Sn is both oxidized and reduced; therefore, the catalyst would be expected to contain a complicated mixture of Pt-Sn, Pt- CeO_x and Pt- SnO_x sites at the surface.

CO Adsorption Microcalorimetry

Figures 6 and 7 show the differential heat of CO adsorption versus coverage at 298 K for catalysts reduced at 473 and 773 K. As the CO coverage increases, the differential heat of adsorption decreases due to adsorption on weaker sites and/or interactions between adsorbed species. At higher coverage, the significant decrease in the differential heat of adsorption indicates saturation of the surface. In the case of Pt/ Al_2O_3 (Figure 6a) the initial differential heat was 140 kJ/mol for the catalyst reduced at 473 K. This value is in good agreement with other studies of CO adsorption on

alumina-supported platinum catalysts [38]. Adsorption heat decreased until a coverage of $20 \mu\text{mol CO g}^{-1}$, where a plateau around 120 kJ/mol was observed. Reduction at higher temperature caused a decrease in initial heat (from 140 to 120 kJ/mol) which was maintained over a wide range of surface coverage before a drastic fall to the weakly adsorbed CO (70 kJ/mol). This finding indicates a higher homogeneity of the surface metal atoms for CO adsorption when catalyst is reduced at 773 K , while the higher initial heat of adsorption obtained in the sample reduced at low temperature could be attributed to the interaction of CO with highly unsaturated metal atoms at corners and edges [38]. Reduction at higher temperatures decreased the CO saturation coverage from 55 to $45 \mu\text{mol CO g}^{-1}$ as reported in Table 4. This effect could be due to sintering of the Pt particles after high temperature reduction, and this change was not observed with XPS.

No change in the initial heats (140 kJ/mol) was observed for the Pt-Sn/ Al_2O_3 (Figure 6b) catalyst after reduction at 773 K , probably because active sites placed in corners and edges have been already covered by tin after reduction at low temperature. The adsorption heat-coverage profile was similar for the catalysts reduced at 473 and 773 K until about $20 \mu\text{mol CO/g}$. However, reduction at 773 K caused a strong decrease in the saturation coverage value from 49 to $32 \mu\text{mol CO/g}$ (also detected by XPS), in agreement with other Pt-Sn (1:1) microcalorimetric studies [15,23,39]. Since Mössbauer results indicate the presence of Pt-Sn alloy after reduction at 773 K , one could expect to find changes in initial adsorption heats of CO on platinum. However, it has been shown that Pt-Sn catalysts prepared by sequential impregnation techniques can lead to a large fraction of unalloyed platinum [40]. In addition, for changes in the initial heats of adsorption to be observed, a larger fraction of Pt-Sn alloy formation is needed [15].

Pt/ CeO_2 - Al_2O_3 (Figure 7a) showed higher initial heats (from 123 to 143 kJ/mol) and a decrease in the CO saturation coverage (from 55 to $33 \mu\text{mol CO/g}$, Table 4) when reduced at high temperature. In addition, the differential heat of CO adsorption strongly decreases with coverage, indicating a heterogeneous distribution of adsorption sites. This behavior could be due to decoration of the Pt metal with reduced ceria oxide (CeO_x). This decoration effect could also explain the inhibition of the chemisorption capacity of platinum detected by microcalorimetry and the XPS results for Pt/Al and Pt/Ce. This geometric effect would reduce the number of accessible platinum particles but, at the same time, produce the appearance of new Pt- CeO_x sites at the metal-support

interface [4]. As discussed by Bernal, et al. decoration of ceria usually occurs at higher reduction temperature (973 K) than used here for Pt/CeO₂ catalysts [4]. However these results are based on catalysts supported on ceria instead of ceria supported alumina. It is interesting to remark (Table 4) that cerium addition produced an increase in the CO/Pt ratio after reduction at 473 K (from 0.57 in Pt/Al₂O₃ to 0.75 in Pt/CeO₂-Al₂O₃). This fact could be due to the additional adsorption of CO on ceria, leading to a higher amount of adsorbed CO.

Pt-Sn/CeO₂-Al₂O₃ (Figure 7b) showed similar heat-coverage profile at both reduction temperatures. The saturation coverage decreased slightly from 27 to 24 μmol CO/g (Table 4) as the reduction temperature increased from 473 to 773 K. Note that the addition of both Sn and CeO₂ decreases the number of Pt surface sites. When only Sn or CeO₂ is added to Pt a high temperature reduction is needed to cause a decrease in Pt surface area. However, when both Sn and CeO₂ are added to the catalyst a synergistic effect is seen where the Pt surface area is significantly lower at a reduction temperature of 473 K. This effect is probably due to the ability of the Sn to increase the reducibility of CeO₂, thus causing the decoration effect to occur at a lower reduction temperature.

Catalytic Behavior

The performance of the catalysts was tested for hydrogenation of crotonaldehyde. The behavior was similar in all cases: after the first stages of reaction (approximately 25 min. on stream) the activity decreased to a stable value which was similar for all catalysts. The deactivation of the catalyst has been attributed to decarbonylation of the reactant molecule yielding carbon monoxide, which is irreversible adsorbed on platinum at the reaction conditions [41]. Although no appreciable differences were found in steady state activities for the different catalysts, interesting results were obtained in initial activities. Figure 8 shows the initial overall activity (micromoles of crotonaldehyde reacted per micromoles of platinum per second) of the catalysts under study for both 473 and 773 K reduction temperatures. The reported activity values are reported only when a carbon balance was achieved (i.e., once the amount of crotonaldehyde leaving the reactor matched that fed minus that transformed into products). For catalysts reduced at low temperature the initial activity follows the order: Pt/CeO₂-Al₂O₃ > PtAl₂O₃ > Pt-Sn/CeO₂-Al₂O₃ > Pt-Sn/Al₂O₃. Using the value of activity for unpromoted Pt/Al₂O₃ as a reference, the higher activity found in Pt/CeO₂-Al₂O₃ indicates that cerium is already able to promote platinum at even a low

reduction temperature. However tin decreased the initial activity which could be due to the partial blocking of platinum sites by tin.

Reduction at 773 K produced an increase in the initial activity in all cases, with the initial activity decreasing in the following order: Pt/CeO₂-Al₂O₃ > PtAl₂O₃ > Pt-Sn/Al₂O₃ > Pt-Sn/CeO₂-Al₂O₃. In the case of the unpromoted Pt/Al₂O₃ catalyst, the observed increase in activity after reduction at high temperature is probably not due to changes in particle size, since XPS results indicate constant Pt/Al atomic ratio (Table 2) with reduction temperature. However, the high temperature reduction treatment changes the energetic distribution of platinum sites for CO adsorption (Figure 6a). The higher homogeneity found in the heat-coverage profile for CO adsorption after reduction at 773 K could indicate a possible superficial redistribution of the platinum exposed faces: from an open faces or steps after reduction at 473 K to a higher number of dense (111) faces more favorable for crotonaldehyde hydrogenation [42] when reduction temperature increases to 773 K. Furthermore, platinum catalysts supported on non-reducible supports like alumina and silica undergo structural and chemical changes upon reduction at ≥ 773 K [43]. Koningsberger, et al [44] showed that the size of metal clusters in Pt/Al₂O₃ remained stable after reduction at 573 and 723 K but, at the same time, they found important changes in electron d distribution of metal particles as measured by EXAFS. This shift in the d-band distribution after high temperature reduction could account for the enhancement in catalytic activity for the Pt/Al₂O₃ catalyst.

In the case of Pt-Sn/Al₂O₃, the observed promotional effect after reduction at high temperature could be related to either the formation of Pt-Sn alloys or the existence of oxidized tin on platinum particles (Pt-SnO_x). Mössbauer results indicate after reduction at 773 K that 31 % of the tin is alloyed with Pt, 62 % of the Sn is in the Sn(II) state, and 7 % of the Sn is in the Sn(IV) state (Table 3). One proposal for the promotional effect of Sn is that the oxidized metal species act as electrophilic or Lewis acid sites for the adsorption and activation of the C=O bond of crotonaldehyde, via the lone electron pair of the oxygen atom [45]. Therefore, the onset of new Pt-SnO_x sites would explain the observed enhancement in activity during first stages of reaction.

Another proposal for the effects of Sn is that the Sn(II) is associated with the alumina support, and the role of Sn is to form zero-valent PtSn alloy particles, which change the electronic properties of Pt and decreases the size of the surface Pt ensembles (i.e., diluting the Pt surface atoms by forming an alloy) [15,16]. Density functional

studies of ethanol and acetic acid adsorption on Pt and Pt₃Sn alloys showed that the carbon in ethanol or acetic acid binds only to Pt surface sites, whereas the oxygen in ethanol or acetic acid binds to either Pt or Sn surface sites. This theory is also consistent with results from Jerdev, et al. who observed that model Sn/Pt(111) surfaces formed PtSn alloys which were twice as active as Pt(111) surfaces for hydrogenation of crotonaldehyde [46]. Jerdev, et al. observed that oxidic Sn species were not stable under reaction conditions.

In the case of Pt/CeO₂-Al₂O₃ the observed enhancement in initial activity could involve two effects: the decoration of metal particles by partially reduced ceria and the creation of new sites at the metal-support interface that are effective for activation of the carbonyl bond. For the Pt-Sn/CeO₂-Al₂O₃ catalyst the initial activity of the catalyst increases as the reduction temperature increases. From the characterization studies the higher reduction temperature causes an increase in the amount of reduced cerium (which would lead to more decoration of the Pt particles) and an alloying of the Sn and Pt.

The products obtained under the conditions used in this study are butyraldehyde (formed by the hydrogenation of the C=C bond), crotyl alcohol (but-2-en-ol, formed by the hydrogenation of the carbonyl C=O bond), butanol (formed upon the hydrogenation of the primary products butyraldehyde and crotyl alcohol), and the light hydrocarbon butane (formed through butanol hydrogenation). The selectivity to crotyl alcohol (molar fraction %) as a function of the time on stream at 353 K after reduction at both low (473 K) and high (773 K) temperature is plotted in Figures 9 and 10. The selectivity to crotyl alcohol for catalysts reduced at 473 K decreased in the order of Pt-Sn/CeO₂-Al₂O₃ > Pt/CeO₂-Al₂O₃ ~ Pt-Sn/Al₂O₃ > PtAl₂O₃. Reduction at high temperature produced an increase in selectivity to crotyl alcohol for all catalysts. However, this increase is more pronounced in the case of the promoted catalysts. The selectivity to crotyl alcohol for catalysts reduced at 773 K decreases according to Pt-Sn/CeO₂-Al₂O₃ > Pt/CeO₂-Al₂O₃ ~ Pt-Sn/Al₂O₃ >> PtAl₂O₃.

Pt/Al₂O₃ exhibited a low selectivity toward crotyl alcohol (less than 8 %) as expected for the unpromoted catalyst (Figure 9a), and increasing the reduction temperature only caused a minor increase in crotyl alcohol selectivity. Reduction of this catalyst at 773 K caused some sintering, which could result in a surface redistribution of platinum exposed faces toward a higher number of (111) crystal planes. These close-packed metal faces are not favourable for the C=C coordination and a greater

participation of this face in the catalyst surface can improve the selectivity to crotyl alcohol [42]

In the case of promoted catalysts, Pt-Sn-CeO_x interactions can modify the adsorption mode of crotonaldehyde on platinum particles. These interactions increase as the reduction temperature increases as shown by XPS, microcalorimetry, and ¹¹⁹Sn Mössbauer studies. DFT, microcalorimetry, and infrared studies of Pt and Pt₃Sn alloys with oxygenates, indicate both an electronic and geometric effect of Sn addition to Pt [31]. This modification also could explain the origin of the selectivity enhancement observed for the Sn-promoted catalysts for crotonaldehyde hydrogenation. A higher electronic density on platinum atoms creates a weaker interaction of the C=C bond of crotonaldehyde, favoring adsorption via the C=O bond, leading to a higher selectivity toward crotyl alcohol [45]. This higher electron density is formed by the creation of PtSn, Pt-SnO_x and Pt-CeO_x (Pt decorated with CeO_x) sites that are able to activate the carbonyl bond of the crotonaldehyde molecule. Poisoning of these sites by strong adsorption of reactant and/or products would be the origin of the observed loss of selectivity with time on stream, which is also accompanied by the decrease in the overall activity.

4. CONCLUSIONS

This study shows that addition of Sn (in a Pt/Sn 1:1 atomic ratio) and/or CeO₂ to Pt/Al₂O₃ catalysts improves the selectivity to crotyl alcohol during crotonaldehyde hydrogenation. Ceria addition to Pt/Al₂O₃ improves the initial activity for crotonaldehyde hydrogenation, whereas Sn addition (in the amount used in this study) to Pt/Al₂O₃ or Pt/CeO₂-Al₂O₃ decreases the catalytic activity. XPS and ¹¹⁹Sn Mössbauer spectroscopy results show that reduction of tin is partially inhibited by the presence of cerium. Moreover the presence of tin facilitates the reduction of cerium. Reduction at 773 K decreases the number of platinum surface sites for the unpromoted and promoted catalysts. The decoration of platinum particles by patches of partially reduced ceria and oxidized tin species or formation of PtSn alloys can account for this loss. This effect produces the onset of new Pt-CeO_x, Pt-SnO_x, and PtSn sites which would explain the observed change in activity for crotonaldehyde hydrogenation. These new sites can selectively interact with the C=O bond of the crotonaldehyde molecule enhancing the selectivity toward crotyl alcohol.

Acknowledgements

Financial support by the Comisión Interministerial de Ciencia y Tecnología (Projects BQU 2000-0467 and BQU 2003-06150) is gratefully acknowledged. J.C. Serrano-Ruiz also thanks Ministerio de Educación y Ciencia (Spain) for its FPI grant. We also acknowledge the contribution made by Dr. F. Coloma in the XPS measurements.

5. REFERENCES

1. S.J. Tauster, S.C. Fung and R.L. Garten, *J. Am. Chem. Soc.* 100 (1978), p. 170
2. A. Dandekar, M. A. Vanicce, *J. Catal.* 183 (1999), 344.
3. D. A. Aranda, M. Schmal, *J. Catal* 171 (1997), 398.
4. Bernal, S.; Calvino, J. J.; Cauqui, M. A.; Gatica, J. M.; Larese, C.; Perez Omil, J. A.; Pintado, J. M., *Catal. Today* 50 (1999), 175.
5. Bernal, S.; Calvino, J. J.; Cauqui, M. A.; Gatica, J. M.; Lopez Cartes, C.; Perez Omil, J. A.; Pintado, J. M., *Catal. Today* 77 (2003), 385.
6. A. K. Datye, D. S. Kalakkad, M., H. Yao, D. J. Smith, *J. Catal.* 155 (1995) 148.
7. C. H. Bartholomew, R. B. Pannel, J. L. Butler, *J. Catal.* 65 (1980) 335.
8. A. Sepúlveda-Escribano, F. Coloma, F. Rodríguez-Reinoso, *J. Catal.* 178 (1998), 649.
9. J. Silvestre-Albero, F. Rodríguez-Reinoso, A. Sepúlveda-Escribano, *J. Catal.* 210 (2002), 127.
10. Abid, M.; Ehret, G.; Touroude, R., *Appl. Catal. A: General* 217 (2001), 219.
11. J. A. Dumesic, S. A. Stevenson, R. D. Sherwood and R. T. K. Baker, *J. Catal.* 99 (1986) 79.
12. D. E. Resasco, R. J. Fenoglio, M. P. Suarez, J. O. Cechini, *J. Phys. Chem.* 90 (1986) 4330.
13. S. Bernal, J. J. Calvino, J. M. Gatica, C. Larese, C. López-Cartes, J. A. Pérez-Omil, *J. Catal.* 169 (1997) 510.
14. M. Abid, V. P. Boncour, R. Touroude, *Appl. Catal. A: General* 297 (2006) 48.
15. R. D. Cortright, J. A. Dumesic, *J. Catal.* 148 (1994) 771.
16. R. D. Cortright, J. M. Hill, J. A. Dumesic, *Catal. Today* 55 (2000) 213.

17. A. Huidobro, A. Sepúlveda-Escribano, F. Rodríguez-Reinoso, *J. Catal.* 212 (2002) 94.
18. F. Coloma, A. Sepúlveda-Escribano, J. L. G. Fierro, F. Rodríguez-Reinoso, *Appl. Catal. A: General* 136 (1996) 231.
19. F. Coloma, A. Sepúlveda-Escribano, J. L. G. Fierro, F. Rodríguez-Reinoso, *Appl. Catal. A: General* 148 (1996) 63.
20. B. E. Spiewak, J. A. Dumesic, *Thermochimica Acta* 290 (1996) 43.
21. B. Riguette, S. Damyanova, G. Goluliev, C. Marques, L. Petrov, J. M. Bueno, J. *Phys. Chem. B* 108 (2004) 5349
22. R. M. Navarro, M. C. Álvarez-Galván, M. C. Sánchez-Sánchez, F. Rosa, J. Fierro, *Appl. Catal. B: Environ.* 55 (2005) 229
23. J. Z. Shyu, K. Otto, *Appl. Surf. Sci.* 32 (1998) 246
24. R. Bouwman, P. Biloen, *J. Catal.* 48 (1977) 209
25. M. J. Tiernan, O. E. Finlayson, *Appl. Catal. B: Environ.* 19 (1998) 23
26. E. Merlen, P. Becat, J. C. Bertolini, P. Delichère, N. Zanier, B. Didillon, *J. Catal.* 159 (1996) 178
27. Weishen, Y., Liwu, L., Yining, F., and Jingling, Z., *Catal. Lett.* 12 (1992), 267.
28. Zhou, Y., and Davis, S. M., *Catal. Lett.* 15 (1992), 51.
29. Bacaud, R., Bussiere, P., and Figueras, F., *J. Catal.* 69 (1981), 399.
30. M. Donders, B. Noorlander, D. van der Vliet, *Bimetallics: Selective Hydrogenation*, April 2004.
31. R. Alcala, J. W. Shabaker, G. W. Huber, M. A. Sanchez-Castillo, J. A. Dumesic, *J. Phys. Chem. B* 109 (2005) 2074.
32. G. Meizner, G. Via, F. Lytle, S. Fung, J. Sinfelt, *J. Phys. Chem.* 92 (1988) 2925
33. A. Caballero, H. Dexpert, B. Didillon, F. Lepeltier, O. Clause, J. Lynch, *J. Phys. Chem.* 97 (1993) 11283
34. C. Vértés, E. Tálas, I. Czako-Nagy, J. Ryczkowski, S. Göbölös, A. Vértés, J. Margitfalvi, *Appl. Catal.* 68 (1991) 149
35. G. Del Angel, A. Bonilla, Y. Peña, J. Navarrete, J. Fierro, D.R. Acosta, *J. Catal.* 219 (2003) 63
36. A. Laachir, V. Perrichon, A. Badri, J. Lamotte, E. Catherine, J. C. Lavalley, J. El Fallal, L. Hilaire, F. le Normand, E. Quéméré, G. N. Sauvion, O. Touret, *J. Chem. Soc. Faraday Trans.* 87 (1991) 1601

37. M.S.P. Mastelaro, V. R. Nascente, A.O.A. Florentino, *J. Phys. Chem B* 105 (2001), 10515.
38. A. Guerrero-Ruiz, A. Maroto-Valiente, M. Cerro-Alarcón, B. Bachiller-Baeza, I. Rodriguez-Ramos, *Topics in Catalysis*, 19 (2002) 303
39. H. Lieske, J. Volter, *J. Catal.* 90 (1984), 46.
40. S.M. Stagg, C.A. Querini, W. E. Alvarez, D. E. Resasco, *J. Catal.* 168 (1997), 75.
41. M. English, A. Jentys, J. A. Lercher, *J. Catal.* 166 (1997), 25.
42. F. Delbeq, S. Sautet, *J. Catal.* 152 (1995) 217
43. G.J. den Otter, F. M. Dautzenberg, *J. Catal.* 53 (1978), 116.
44. D. C. Koningsberger, M. Vaarkamp, *Physica B: Condensed Matter* 208-209 (1995), 633.
45. P. Gallezot, D. Richard, *Catal. Rev. Sci. Eng.* 40 (1998), 81.
46. D. I. Jerdev, A. Olivas, B. E. Koel, *J. Catal.* 205 (2002) 278.
47. P. Beccat, J. C. Bertolini, Y. Gauthier, J. Massardier, P. Ruiz, *J. Catal.* 126 (1990) 451.

Figure captions

Table 1. Summary of Catalysts Composition

Table 2. Catalysts characterization by XPS

Table 3. ^{119}Sn Mössbauer Parameters of Pt-Sn Catalysts at 300K

Table 4. CO uptake and CO/Pt ratios for catalysts reduced at both 473 and 773 K.

Figure captions

Figure 1. XPS Pt 4d_{5/2} spectra of the calcined (unreduced) catalyst

Figure 2. XPS Pt 4d_{5/2} spectra of the calcined (unreduced) and reduced Pt/CeO₂-Al₂O₃ catalyst

Figure 3. XPS Sn 3d_{5/2} spectra of the calcined (unreduced) and reduced catalysts. a) Pt-Sn/Al₂O₃; b) Pt-Sn/CeO₂-Al₂O₃

Figure 4. % Ce (III) as a function of the reduction temperature. (open Symbols) Pt/CeO₂-Al₂O₃; (solid symbols) Pt-Sn/CeO₂-Al₂O₃.

Figure 5. ^{119}Sn Tin Mössbauer spectra for a) Pt-Sn/Al₂O₃ and b) Pt-Sn/CeO₂-Al₂O₃ catalysts after reduction at 473 and 773 K.

Figure 6. Differential heats of carbon monoxide adsorption at 298K on (a) Pt/Al₂O₃ and (b) Pt-Sn/Al₂O₃ catalysts after reduction at 473 K (solid symbols) or 773 K (open symbols)

Figure 7. Differential heats of carbon monoxide adsorption at 298K on (a) Pt/CeO₂-Al₂O₃ and (b) Pt-Sn/CeO₂-Al₂O₃ catalysts after reduction at 473 K (solid symbols) or 773 K (open symbols)

Figure 8. Initial catalytic activity for crotonaldehyde hydrogenation at 353 K for catalysts after reduction at 473 or 773 K

Figure 9. Evolution of the selectivity toward crotyl alcohol as a function of the time on stream for the cerium-free catalysts at 353 K, after reduction at 473 (solid symbols) or 773 K (open symbols). (a) Pt/Al₂O₃; (b) Pt-Sn/Al₂O₃.

Figure 10. Evolution of the selectivity toward crotyl alcohol as a function of the time on stream for the cerium-containing catalysts at 353 K, after reduction at 473 (solid symbols) or 773 K (open symbols). (a) Pt/CeO₂-Al₂O₃; (b) Pt-Sn/CeO₂-Al₂O₃.

Catalyst	Pt loading (wt%)	Sn loading (wt%)	Pt/Sn atomic ratio
Pt/Al ₂ O ₃	1.88	----	----
Pt-Sn/Al ₂ O ₃	1.77	1.44	0.74
Pt/CeO ₂ -Al ₂ O ₃	1.43	----	----
Pt-Sn/CeO ₂ -Al ₂ O ₃	1.43	1.19	0.73

Table 1

Catalyst	Red. Temp. (K)	Pt/Al	B.E. Pt $4d_{5/2}$ (eV)	Pt/Sn	Pt/Ce	Ce/Al	% Ce(III)
Pt/Al ₂ O ₃	Unreduced	0.0038	314.3(33), 316.2(49), 317.9(18)	—	—	—	
	473	0.0037	313.0(34), 315.2(45), 317.0(21)	—	—	—	
	773	0.0038	313.0(36), 315.2(45), 317.0(19)	—	—	—	
Pt-Sn/Al ₂ O ₃	Unreduced	0.0045	314.3(32), 316.1(38), 317.9(30)	0.32	—	—	
	473	0.0041	313.5(29), 315.4(42), 317.3(29)	0.29	—	—	
	773	0.0032	313.0(32), 314.8(39), 316.4(29)	0.13	—	—	
Pt/CeO ₂ -Al ₂ O ₃	Unreduced	0.0044	314.8(40), 316.8(41), 318.5(19)	—	0.67	0.0066	20
	473	0.0043	313.5(39), 315.5(44), 317.4(17)	—	0.49	0.0087	37
	773	0.0037	313.1(41), 315.2(43), 317.1(16)	—	0.30	0.0124	39
Pt-Sn/CeO ₂ -Al ₂ O ₃	Unreduced	0.0047	314.8(23), 316.7(45), 318.7(32)	1.33	2.68	0.0017	33
	473	0.0032	313.5(28), 315.4(46), 317.4(26)	0.80	1.61	0.0020	38
	773	0.0037	313.0(33), 315.0(43), 316.8(24)	0.49	1.35	0.0027	46

Table 2

Catalyst	Reduct. Temp. (K)	Isomer Shift (mm s ⁻¹)	Quadrupole Splitting (mm s ⁻¹)	Relative Area (%)	Chemical form of Sn	Average Sn State
Pt-Sn/Al ₂ O ₃	473	0.03	0.63	80	Sn(IV)	3.6
		2.55	1.60	20	Sn(II)	
	773	2.33	0.00	31	Pt-Sn Alloy	1.5
		2.71	2.22	62	Sn(II)	
		0.50	0.00	7	Sn(IV)	
Pt-Sn/CeO ₂ -Al ₂ O ₃	473	0.00	0.60	93	Sn(IV)	3.9
		2.87	1.56	7	Sn(II)	
	773	2.19	0.00	21	Pt-Sn Alloy	1.7
		2.67	2.30	71	Sn(II)	
		0.50	0.00	8	Sn(IV)	

Table 3

Catalyst	Reduct. Temp. (K)	CO uptake ($\mu\text{mol CO} \cdot \text{g}^{-1}$)	CO/Pt
Pt/Al ₂ O ₃	473	55	0.57
	773	45	0.47
Pt-Sn/Al ₂ O ₃	473	49	0.54
	773	32	0.35
Pt/CeO ₂ -Al ₂ O ₃	473	55	0.75
	773	33	0.45
Pt-Sn/CeO ₂ -Al ₂ O ₃	473	27	0.37
	773	24	0.33

Table 4

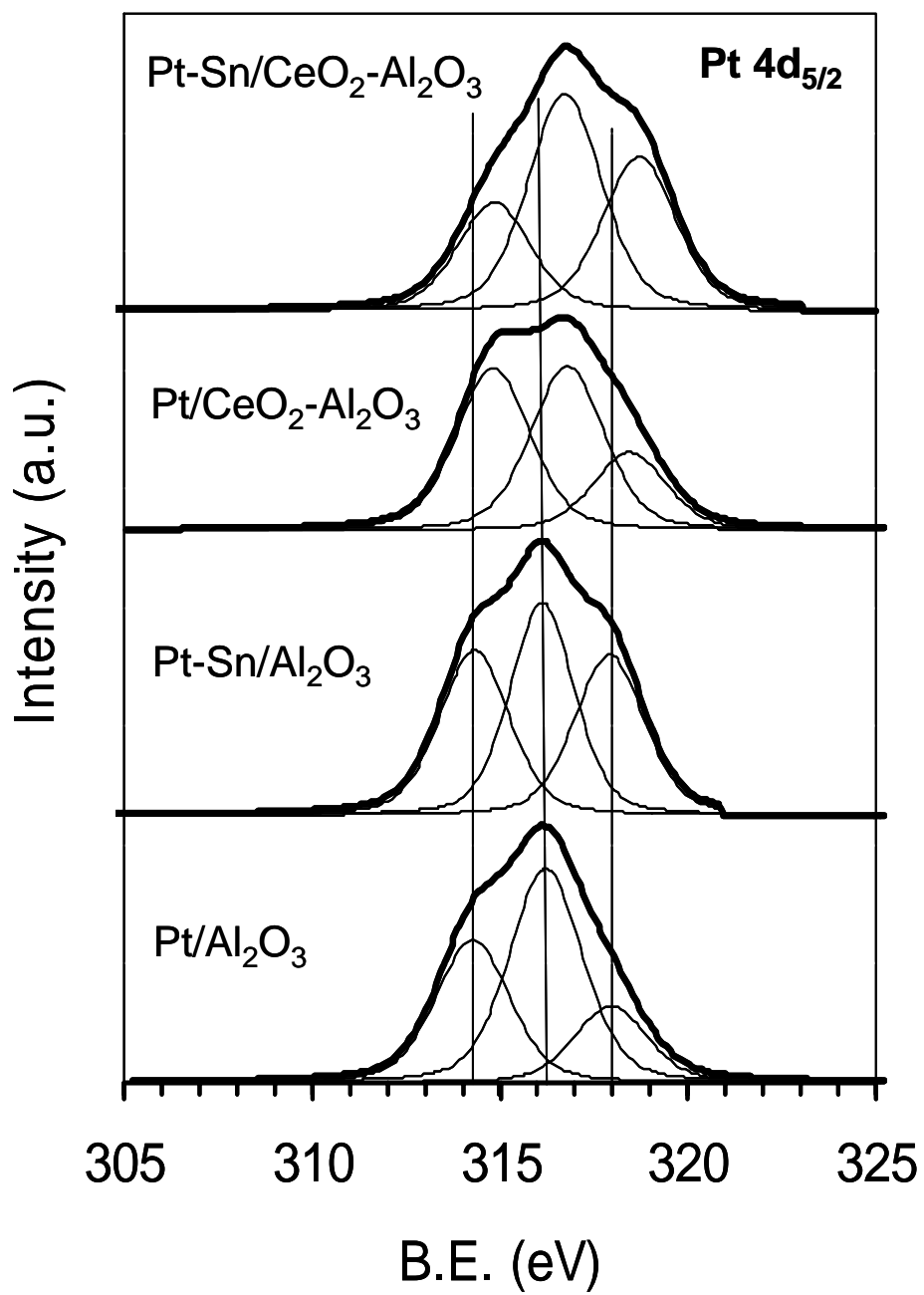


Figure 1

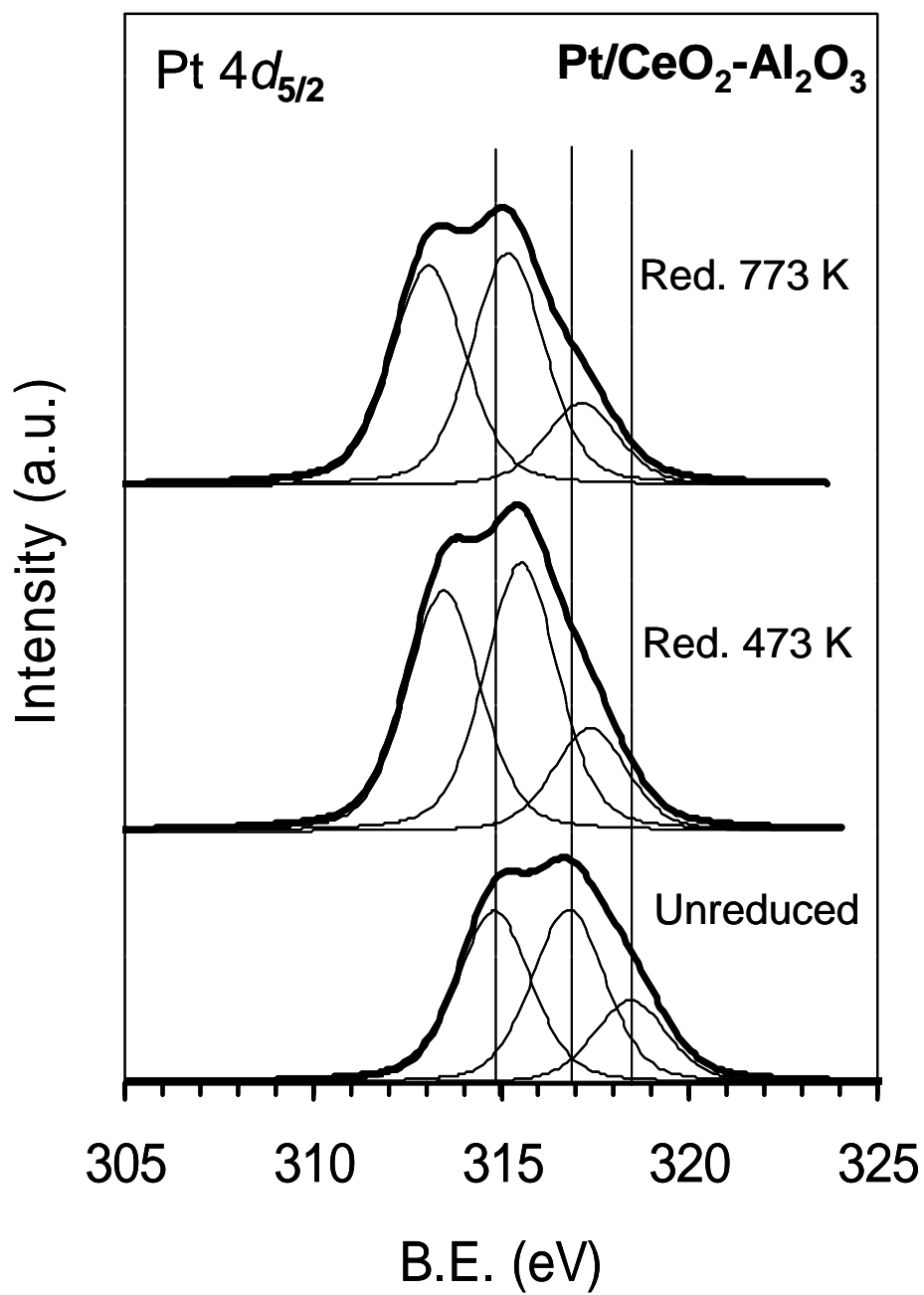


Figure 2

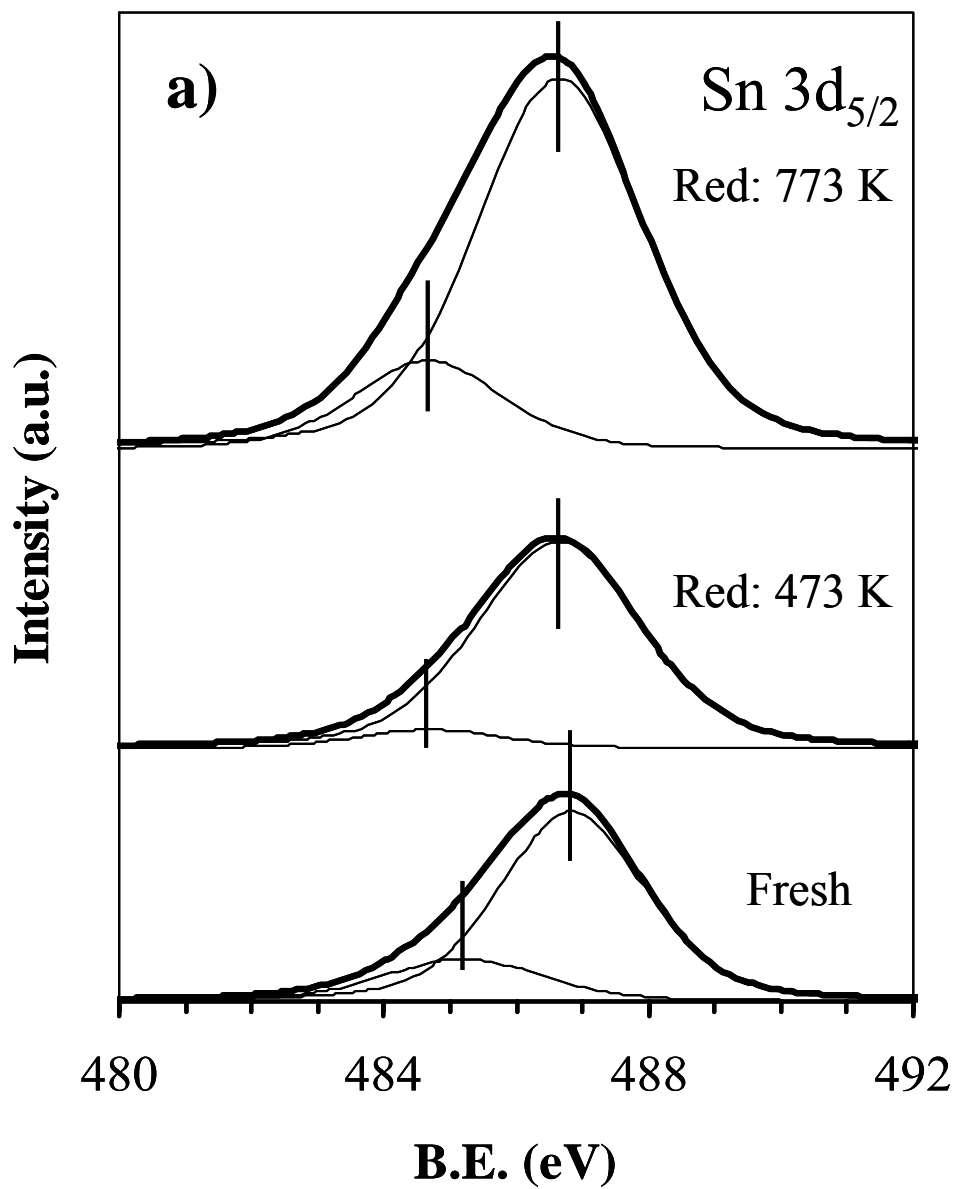


Figure 3a

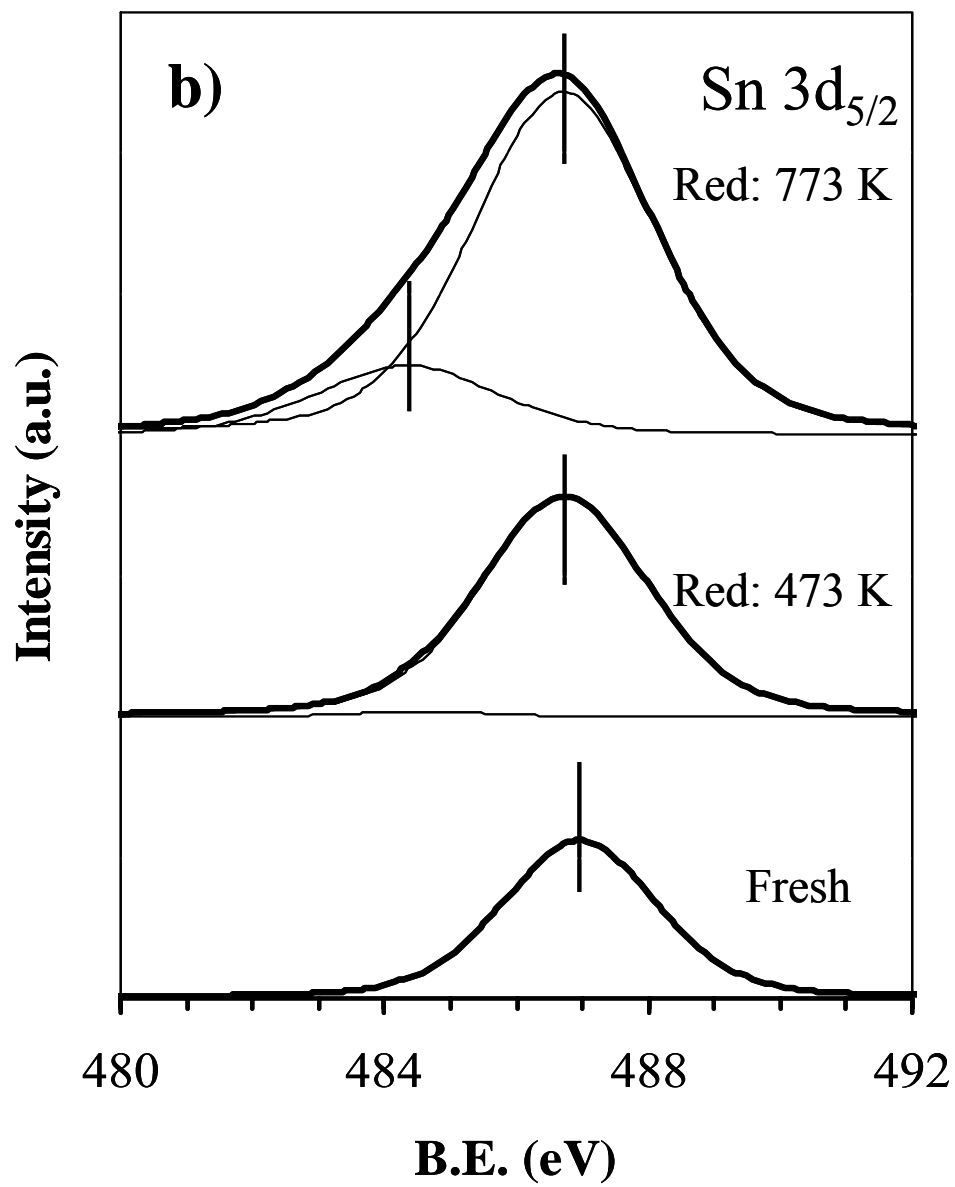


Figure 3b

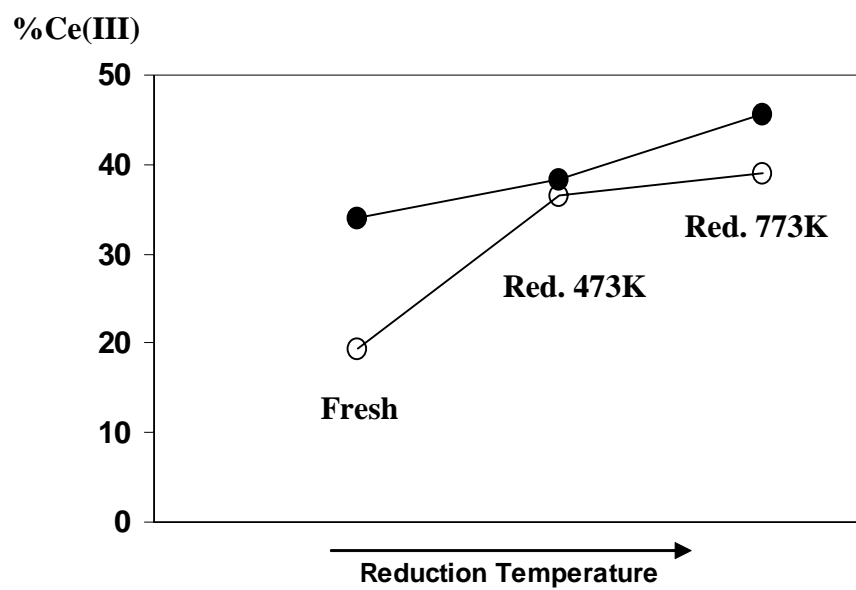


Figure 4

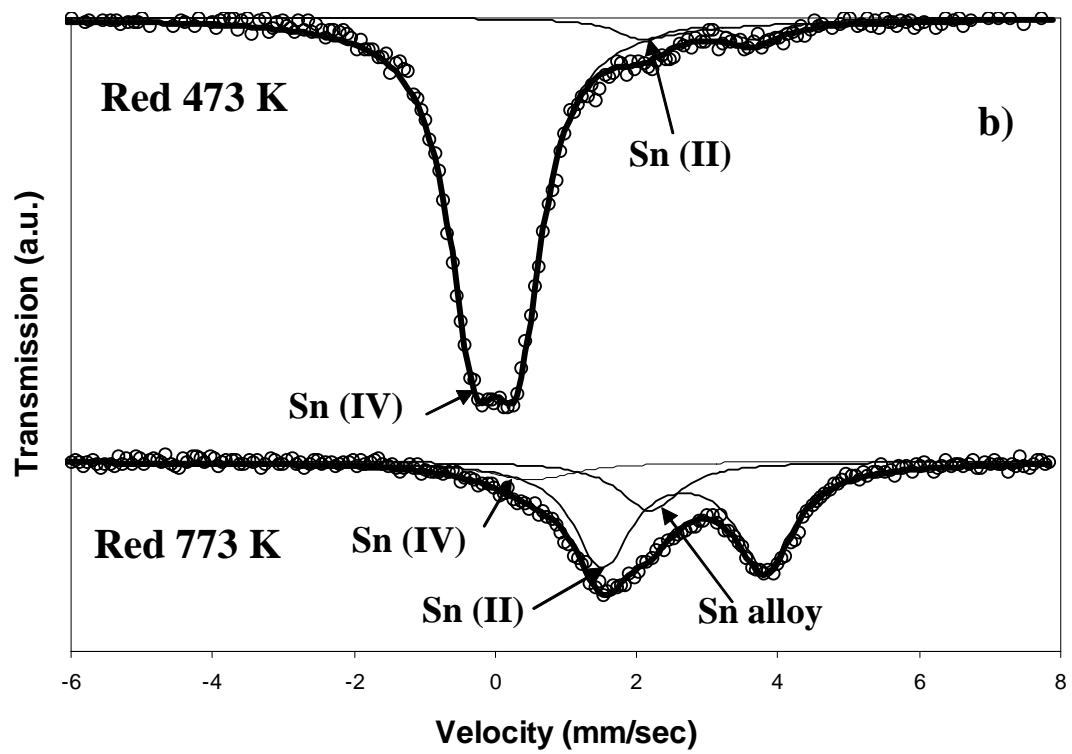
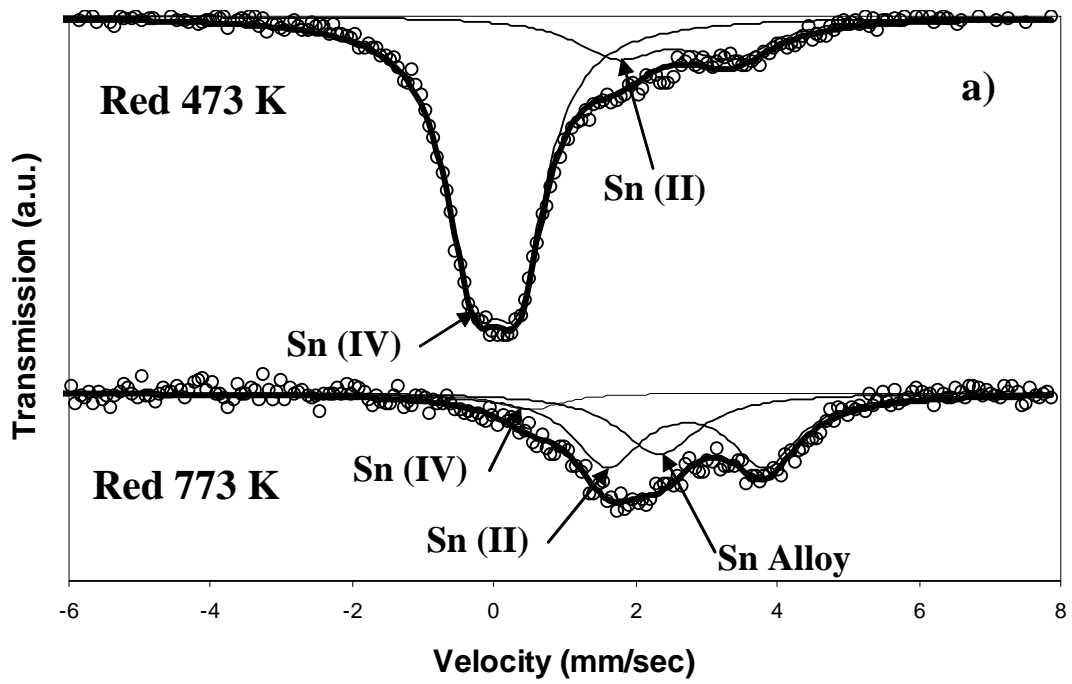


Figure 5

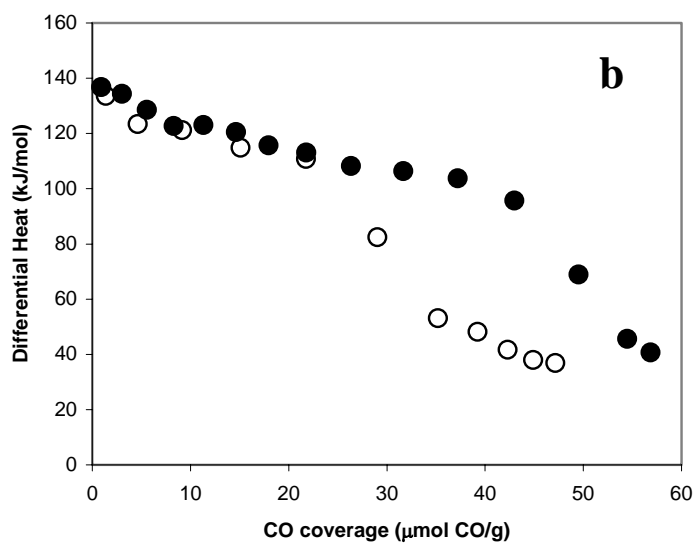
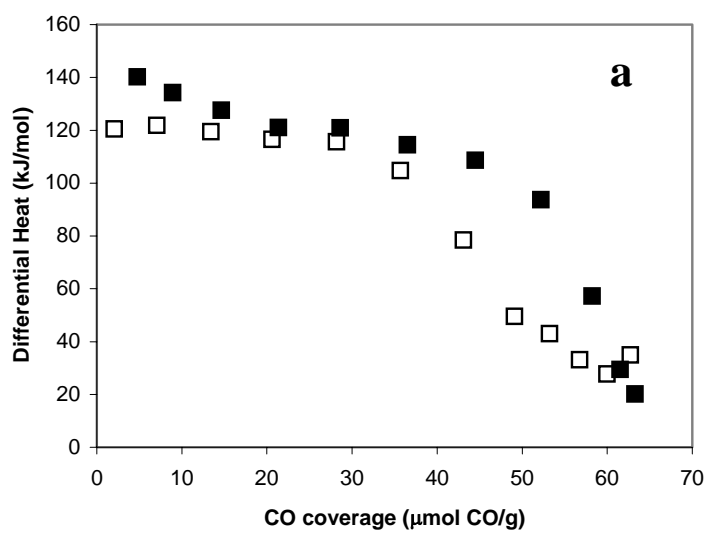


Figure 6

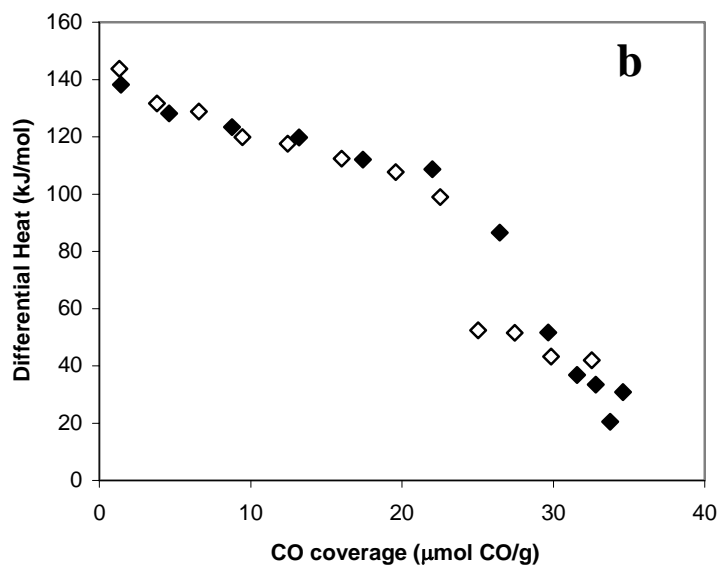
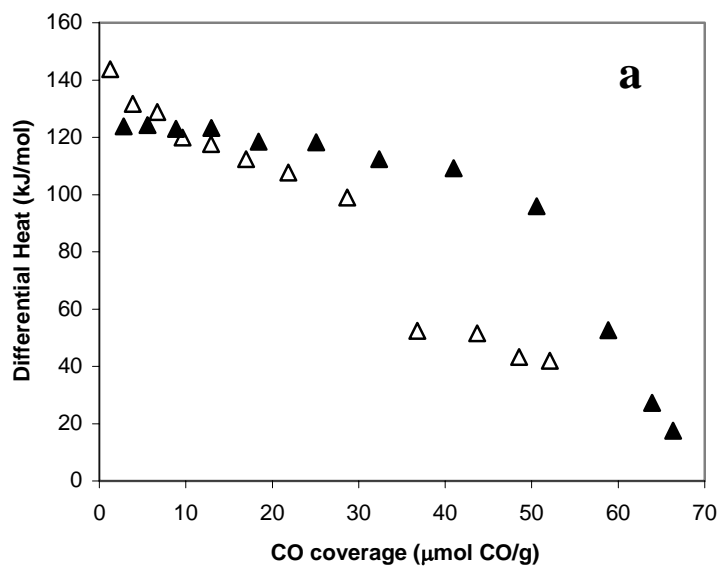
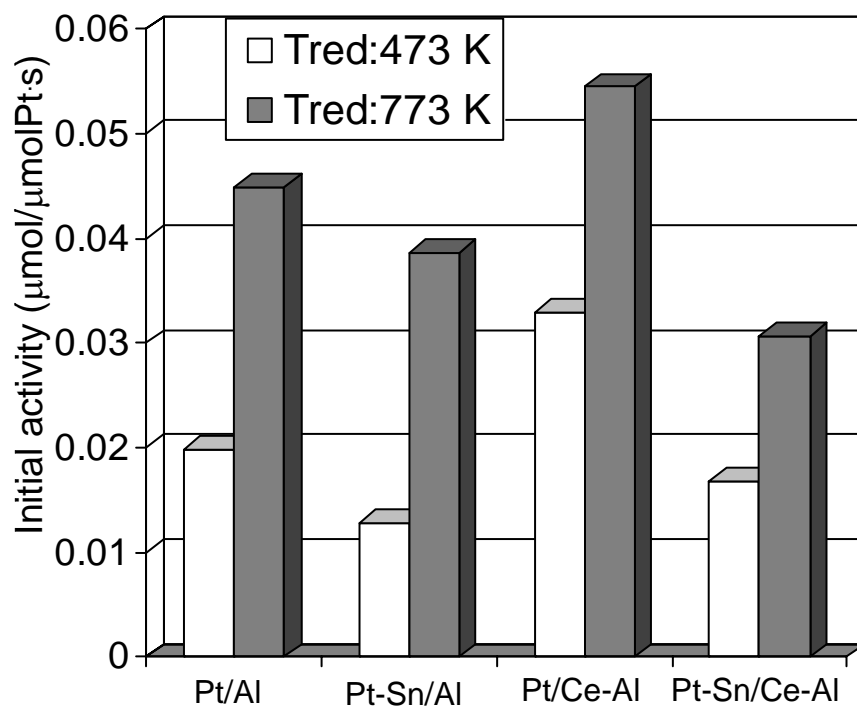


Figure 7



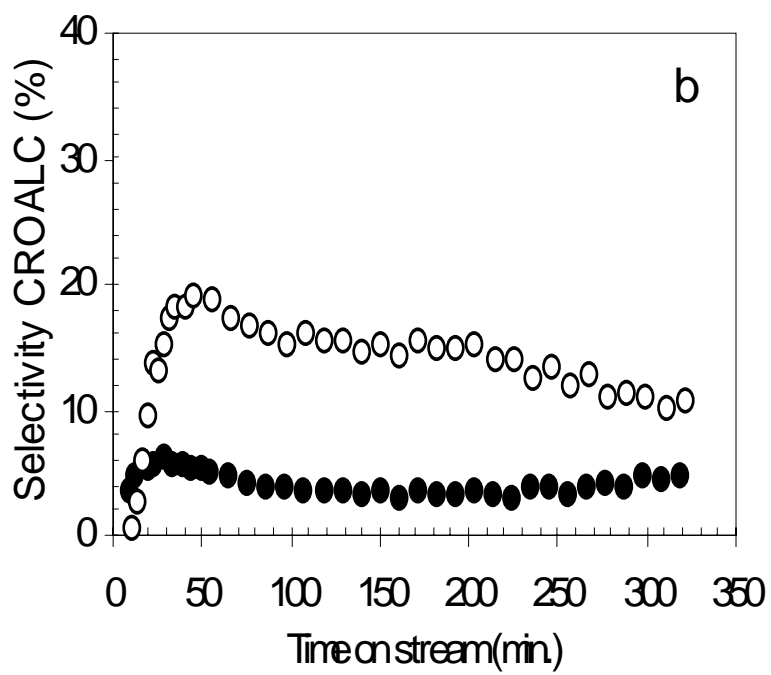
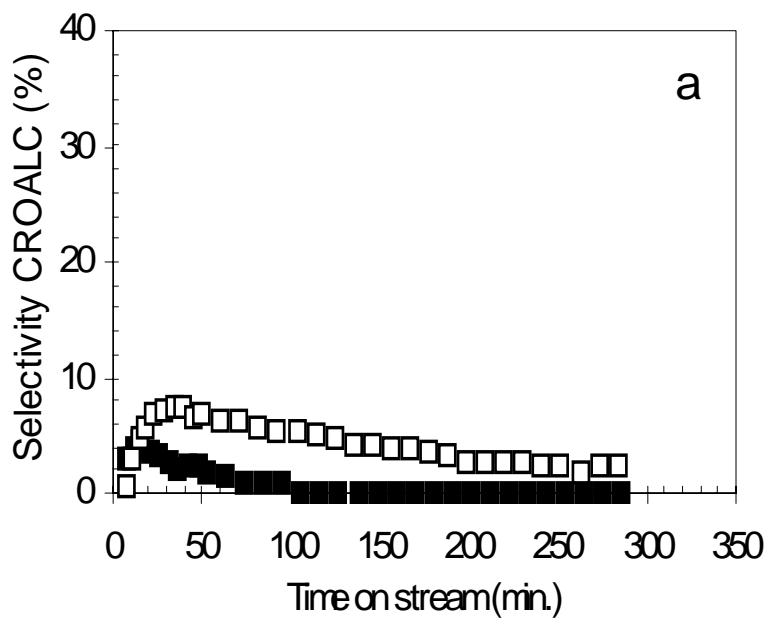


Figure 9

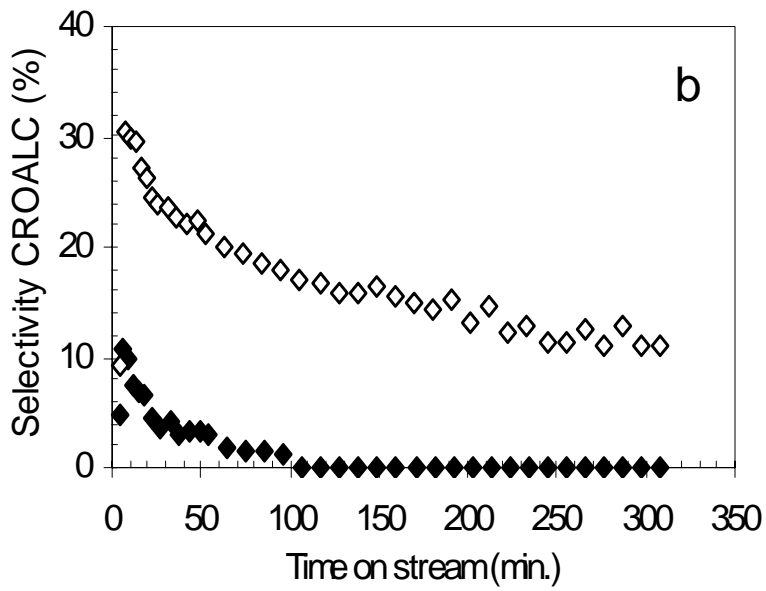
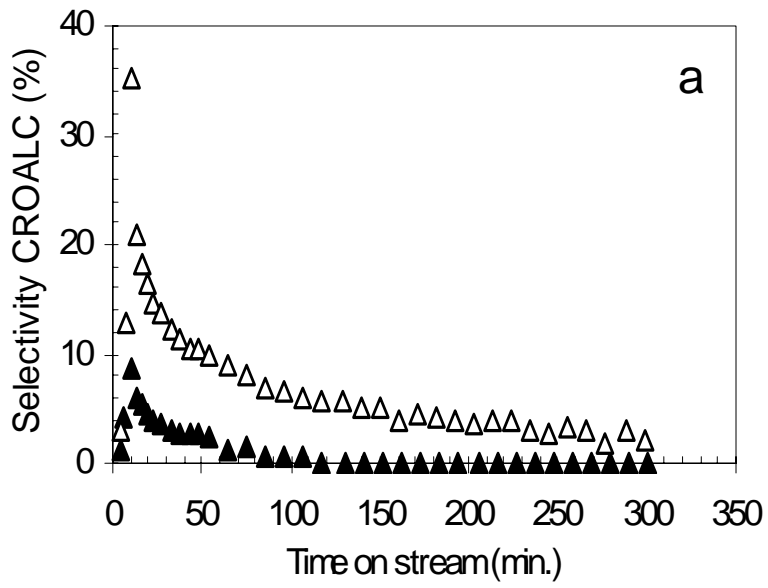


Figure 10